International Journal of Enhanced Research in Science Technology & Engineering, ISSN: 2319-7463
Vol. 3 Issue 9, Sept.-2014, pp: (228-238), Impact Factor: 1.252, Available online at: www.erpublications.com

A Unified Dynamic Model for Bi-directional DC-DC Converter

Husam A. Ramadan[1], Yasutaka Imamura[2], Sihun Yang[3], Masahito Shoyama[4]

[1234]Kyushu University, Fukuoka, 819-0395 Japan

Abstract: **This paper presents a unified model for bi-directional DC-DC converters for both directions of power flow. The bi-directional DC-DC converter is analyzed using a seamless dynamic model with an independent voltage source and an independent current source, which polarity depends on the direction of the power flow. A small signal model is derived using a state space averaging method. Furthermore, the transient response and the frequency characteristics are discussed. Example circuits for bi-directional DC-DC converter are investigated analytically, using simulation, and experimentally.**

Keywords: DC-DC converter, bi-directional, dynamic model, seamless, state space averaging.

1. Introduction

Nowadays, a system uses various types of energy sources has been sought after, and a hybrid system based on fuel cells and super-capacitors as an environmentally renewable energy system has been applied in many fields, such as hybrid electric vehicle (HEV), uninterruptible power supply (UPS) and so on [1]-[6]. In these systems, bi-directional DC-DC converters play a key role. For example, in power system of electric vehicle, batteries are connected to load/source modules through bi-directional DC-DC converters for ensuring a stable energy supply (see Fig.1). Another example, configuration of EMS (Energy Management System) is shown in Fig. 2. A battery is connected between load modules and source modules through bi-directional DC-DC converter. The fluctuation nature of most renewable-energy sources, like wind and solar, makes them unsuitable for standalone operation. Thus, bi-directional DC-DC converter and battery are needed to manage this system. Therefore, the bi-directional DC-DC converter is one of the most important topics in power electronics [7]-[8].

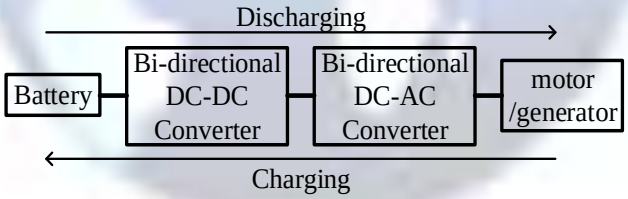

Fig. 1.Configuration of power system in electric vehicle.

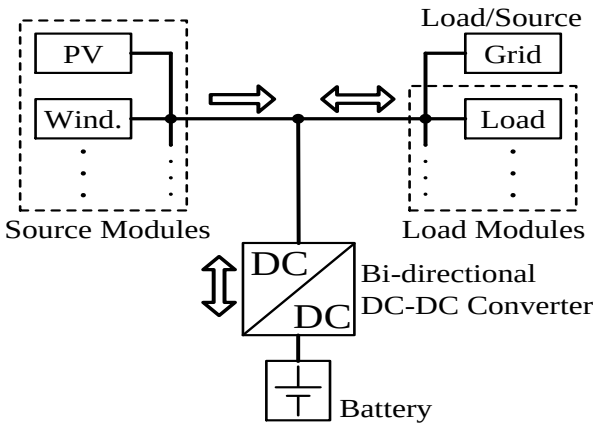

Fig.2. Configuration of EMS

Bi-directional DC–DC converters allow transfer of power between two dc sources, in either direction. Due to their ability to reverse the direction of flow of current, and thereby power, while maintaining the voltage polarity at either end unchanged. Bi-directional DC-DC converter has two operating modes as shown in Fig. 3, and they are frequently exchanged to smooth a power. These two modes are: 1- Charging mode: The power is sent from the battery to load/source modules when load/source modules need the power. 2- Charging mode: The power is sent from the load/source modules to battery when load/source modules have enough amount of the power.

By using conventional modeling method [9], different model is needed for each power direction (each operation mode), as shown in Fig. 4. Furthermore, the control loop also should be changed according to the direction of the power flow. Therefore, analyzing and controlling of bi-directional DC-DC converter are complex.

For the sake of solving this problem, a seamless dynamic model of a bi-directional DC-DC converter is proposed in this paper. This model is derived using a state space averaging method [10]-[12]. As shown in Fig.5, an independent voltage source represents the battery, and an independent bi-polar current source represents the load/source modules. The polarity of the bi-polar current source decides the direction of the power flow. Herein, only the voltage of the bi-polar current source is sensed and controlled. Hence, the control loop doesn't need to be switched according to the direction of the power flow. In other words, a simple analyzing and controlling of bi-directional DC-DC converter can be fulfilled via this seamless model.

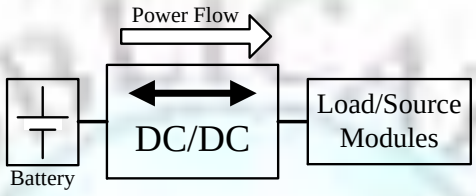

(a) Discharging mode

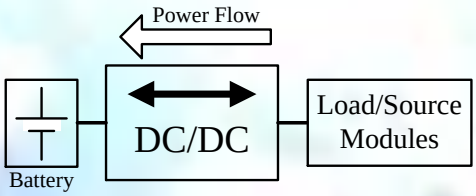

(b) Charging mode.

Fig.3. Operating mode of bi-directional DC-DC Converter.

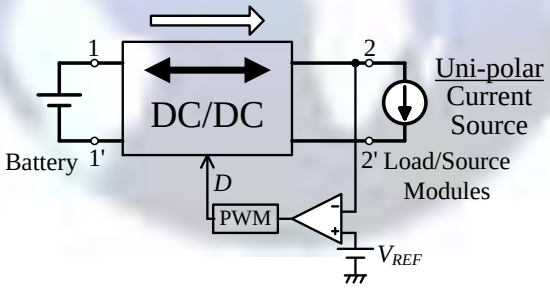

(a) Discharging mode.

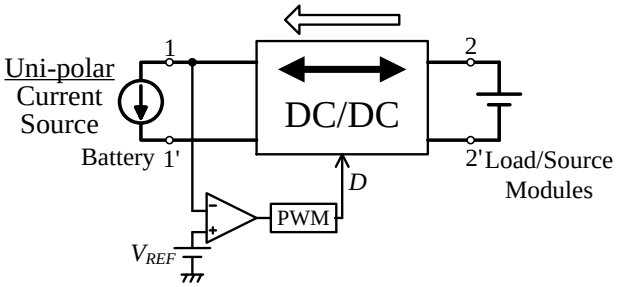

(b) Charging mode.

Fig.4. Conventional circuit model of bi-directional DC-DC converter.

International Journal of Enhanced Research in Science Technology & Engineering, ISSN: 2319-7463
Vol. 3 Issue 9, Sept.-2014, pp: (228-238), Impact Factor: 1.252, Available online at: www.erpublications.com

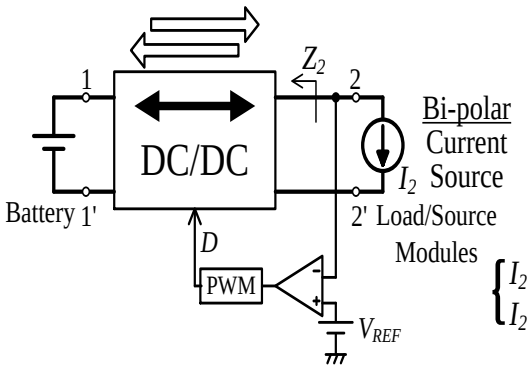

(2)

Fig.5. Proposed seamless circuit model of bi-directional DC-DC converter.

2. Circuit Topology

Seamless dynamic models based on two circuit topologies are analyzed and compared, herein. These two circuit topologies are shown in Fig. 6 and Fig. 7. Figure 6 presents a buck-based circuit topology, however Fig. 7 introduces a boost-based circuit topology. In Fig. 6 and Fig.7, the current source side voltage v_2 is considered a control variable, and duty ratio d of the mean switch S_M is considered an input variable. The current source side voltage v_2 is observed and duty ratio d is controlled by the control circuit. Also, the synchronous switchS_S, with a duty ratio d' (=1-d), has a complementary state with the main switch S_M.

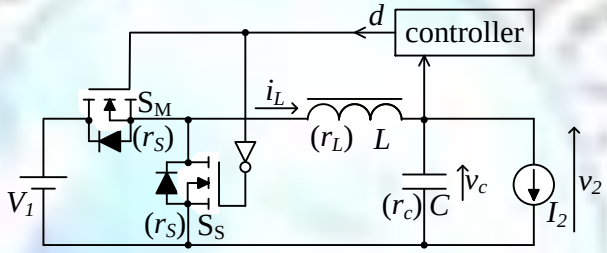

Fig.6.Circuit topology of buck-based type.

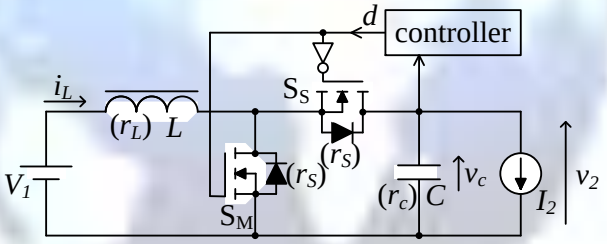

Fig.7. Circuit topology of boost-based type.

3. Seamless Averaged Model

Considering the state-space vector $\boldsymbol{x}(t) = [i_L(t) \quad v_c(t)]^T$ and the input vector$\boldsymbol{u} = [V_1 \quad I_2]^T$, the state space equations at state 1 and state 2 become:

State 1 (S_M : ON, S_S : OFF)

$$\frac{d\boldsymbol{x}}{dt} = \boldsymbol{A_1 x} + \boldsymbol{B_1 u}, \qquad (1)$$
$$v_2 = \boldsymbol{c_1 x} + \boldsymbol{e_1 u}.$$

State 2 (S_M : OFF, S_S : ON)

$$\frac{d\boldsymbol{x}}{dt} = \boldsymbol{A_2 x} + \boldsymbol{B_2 u}, \qquad (2)$$
$$v_2 = \boldsymbol{c_2 x} + \boldsymbol{e_2 u}.$$

Appling the state-space averaging method for (1) and (2), state equations become:

$$\frac{d\boldsymbol{x}}{dt} = \boldsymbol{Ax} + \boldsymbol{Bu}, \qquad (3)$$

$v_2 = \boldsymbol{cx} + \boldsymbol{eu}$.

where:

$\boldsymbol{A} = d\boldsymbol{A_1} + d'\boldsymbol{A_2}, \quad \boldsymbol{B} = d\boldsymbol{B_1} + d'\boldsymbol{B_2},$
$\boldsymbol{c} = d\boldsymbol{c_1} + d'\boldsymbol{c_2}, \boldsymbol{e} = d\boldsymbol{e_1} + d'\boldsymbol{e_2}.$

Next, on the steady state, circuit parameters are:

$\boldsymbol{U}$	: DC input vector
$\boldsymbol{X}$	: DC state vector
V_2	: DC voltage at current source
D	: DC duty ratio at S_M

The converter waveforms are perturbed at this quiescent operating point:

$\boldsymbol{U}$	$\rightarrow \boldsymbol{U}+\Delta\boldsymbol{u}$
$\boldsymbol{X}$	$\rightarrow \boldsymbol{X}+\Delta\boldsymbol{x}$
V_2	$\rightarrow V_2+\Delta v_2$
D	$\rightarrow D+\Delta D$

where;

ΔD is small ac variations in duty ratio and $\Delta\boldsymbol{u}$is small ac variations in input values. The vectors $\Delta\boldsymbol{x}$and Δv_2 are the resulting small ac variations in the state $\boldsymbol{x}$ and voltagev_2.

The state equations of the small-signal ac model are:

$$\frac{d\boldsymbol{x}}{dt} = \boldsymbol{A}\Delta\boldsymbol{x} + \boldsymbol{B}\Delta\boldsymbol{u} + \boldsymbol{b_p}\Delta D, \qquad (4)$$
$$\Delta v_2 = \boldsymbol{c}\Delta\boldsymbol{x} + \boldsymbol{e}\Delta\boldsymbol{u} + \boldsymbol{e_p}\Delta D.$$

where;

$$\boldsymbol{b_p} = (\boldsymbol{A_1} - \boldsymbol{A_2})\boldsymbol{X} + (\boldsymbol{B_1} - \boldsymbol{B_2})\boldsymbol{U},$$
$$e_p = (\boldsymbol{c_1} - \boldsymbol{c_2})\boldsymbol{X} + (\boldsymbol{e_1} - \boldsymbol{e_2})\boldsymbol{U}.$$

The matrices of$(\boldsymbol{A}), (\boldsymbol{B}), (\boldsymbol{c}), (\boldsymbol{e}), (\boldsymbol{b_p})$, and$(\boldsymbol{e_p})$ are illustrated in Table 1.

From (4), the transfer function G_{dv}(s) between ΔD(s) and Δv_2(s) can be developed, as in (5).

$$G_{dv}(s) = \frac{\Delta V_2(s)}{\Delta D(s)} = \boldsymbol{c}(s\boldsymbol{I} - \boldsymbol{A})^{-1}\boldsymbol{b_p} + e_p \qquad (5)$$

By the same way, the transfer function G_{vv}(s) between ΔV_1(s) and Δv_2(s), and G_{iv}(s) between ΔI_2(s) and Δv_2(s) can be developed as:

(6)

$$G_{vv}(s) = \frac{\Delta V_2(s)}{\Delta V_1(s)} = \{\boldsymbol{c}(s\boldsymbol{I} - \boldsymbol{A})^{-1}\boldsymbol{B} + \boldsymbol{e}\}\begin{bmatrix}1\\0\end{bmatrix} \qquad (7)$$
$$G_{iv}(s) = \frac{\Delta V_2(s)}{\Delta I_2(s)} = \{\boldsymbol{c}(s\boldsymbol{I} - \boldsymbol{A})^{-1}\boldsymbol{B} + \boldsymbol{e}\}\begin{bmatrix}0\\1\end{bmatrix}$$

Table.1. Elements of matrix

Topology	$\boldsymbol{A}$	$\boldsymbol{B}$	$\boldsymbol{c}$	$\boldsymbol{e}$	$\boldsymbol{b_p}$	e_p
Buck	$\begin{bmatrix} -\frac{r_L + r_s + r_c}{L} & -\frac{1}{L} \\ \frac{1}{C} & 0 \end{bmatrix}$	$\begin{bmatrix} \frac{D}{L} & \frac{r_c}{L} \\ 0 & -\frac{1}{C} \end{bmatrix}$	$[r_c \quad 1]$	$[0 \quad -r_c]$	$\begin{bmatrix} \frac{V_1}{L} \\ 0 \end{bmatrix}$	0
Boost	$\begin{bmatrix} -\frac{r_L + r_s + D'r_c}{L} & -\frac{D'}{L} \\ \frac{D'}{C} & 0 \end{bmatrix}$	$\begin{bmatrix} \frac{1}{L} & \frac{D'r_c}{L} \\ 0 & -\frac{1}{C} \end{bmatrix}$	$[D'r_c \quad 1]$	$[0 \quad -r_c]$	$\begin{bmatrix} \frac{1}{D'L}V_1 - \frac{r_L + r_s}{D'L}I_2 \\ -\frac{1}{D'C}I_2 \end{bmatrix}$	$-\frac{r_c}{D'}I_2$

4. Frequency Characteristics

The frequency characteristics of the transfer function G_{dv}(s) is analyzed according to (5), and to the circuit parameters that are listed in Table 1. The equations of transfer function G_{dv}(s) for both buck-based and boost-based type are presented in (8), (9).

$$G_{dv_{buck}}(s) = \frac{(1 + Cr_c s)V_1}{1 + C(r_s + r_L + r_c)s + LCs^2} \tag{8}$$

$$G_{dv_{boost}}(s) = \frac{1}{D'^2 + C(r_L + r_s + D'r_c)s + LCs^2} \times \left\{\left(V_1 - \frac{2(r_L + r_s) + DD'r_c}{D'}I_2\right) + \left(Cr_cV_1 - \frac{Cr_c(r_L + r_s) + L}{D'}I_2\right)s\right\} - \frac{r_c}{D'}I_2 \tag{9}$$

From (8) and (9), it is noticed that the frequency characteristics of the buck-based type don't depend on I_2. Nevertheless, the frequency characteristics of the boost-based type depend on I_2. The frequency characteristics of both buck-based type and boost-based type are analytically and experimentally investigated based on circuit parameters in Table 2.

- For the buck-based type, analytical results are shown in Fig. 8, and experimental results are shown in Fig. 9.According to Fig. 8 and Fig. 9, the frequency characteristics of G_{dv_buck} for both current directions are the same, and they match with (8).These results mean that frequency characteristics of G_{dv_buck}don't depend on the direction of current I_2.

Table 2 Circuit parameters

Symbol	Parameters	Value	
		Buck	Boost
V_1	Voltage at Voltage Source [V]	50	25
I_2	Current at Current Source [A]	-4~4	-2~2
V_2	Voltage at Current Source [V]	25	50
L	Inductance [μH]	120	
C	Capacitance [μF]	100	
r_L	ESR of L [mΩ]	30	
r_C	ESR of C [mΩ]	150	
r_S	On-resistance of switches [mΩ]	150	
f	Switching Frequency [kHz]	100	

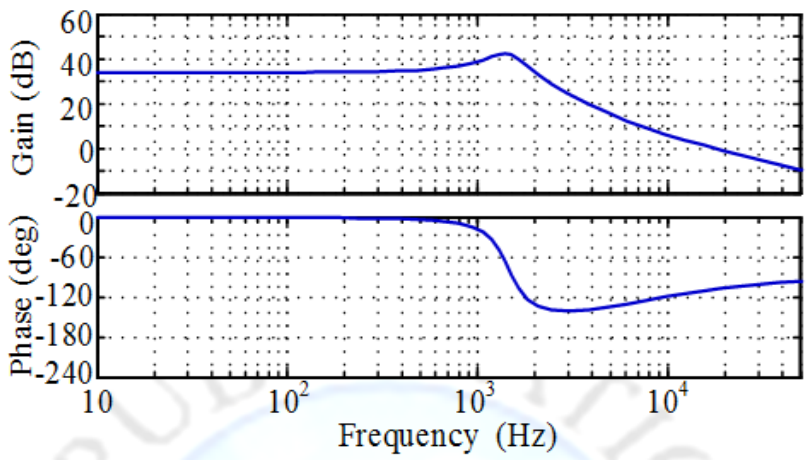

Fig. 8. Frequency characteristics of G_{dv}(analytical results, buck-based type, for any I_2).

- For the boost-based type, analytical results are shown in Fig. 10, and experimental results are shown in Fig. 11. Comparing Fig. 10 (a) and (b), frequency characteristics of G_{dv_boost} don't depend on the direction of current I_2 at low frequency. However, at high frequency, phase plots depend on the direction of current I_2. Stability of the circuit is better when direction of current I_2 is negative. Based on Fig. 10 and Fig. 11, the frequency characteristicsof G_{dv_boost} for both current directionsmatch with (9). These results mean that frequency characteristics of G_{dv_boost} depend on the direction of current I_2.

Comparing the results of the buck-based type with those of the boost-based type; it is found that the buck-based type has an advantage over the boost-based typeon designing the controller; since its frequency characteristics don't depend on current I_2.

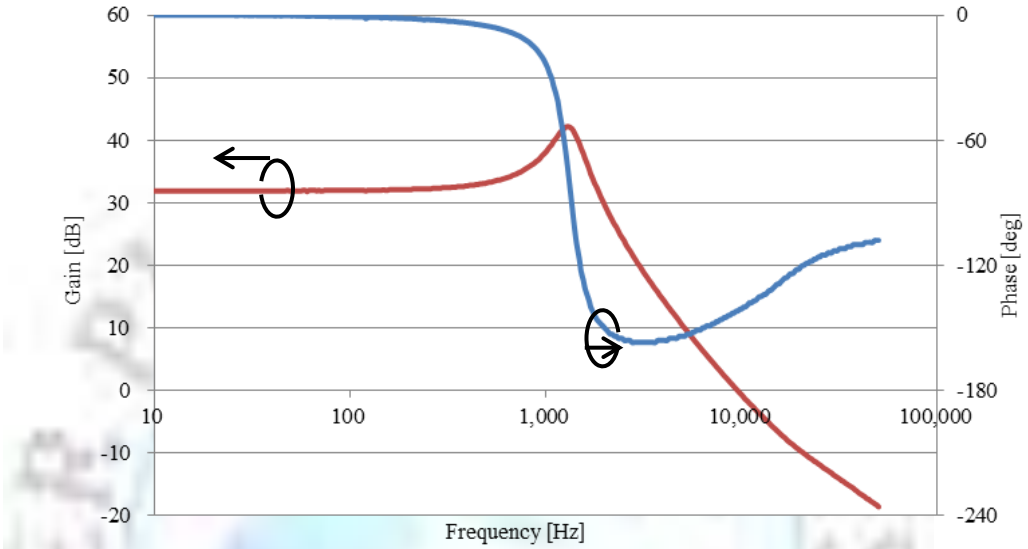

(a) I_2= +4 A

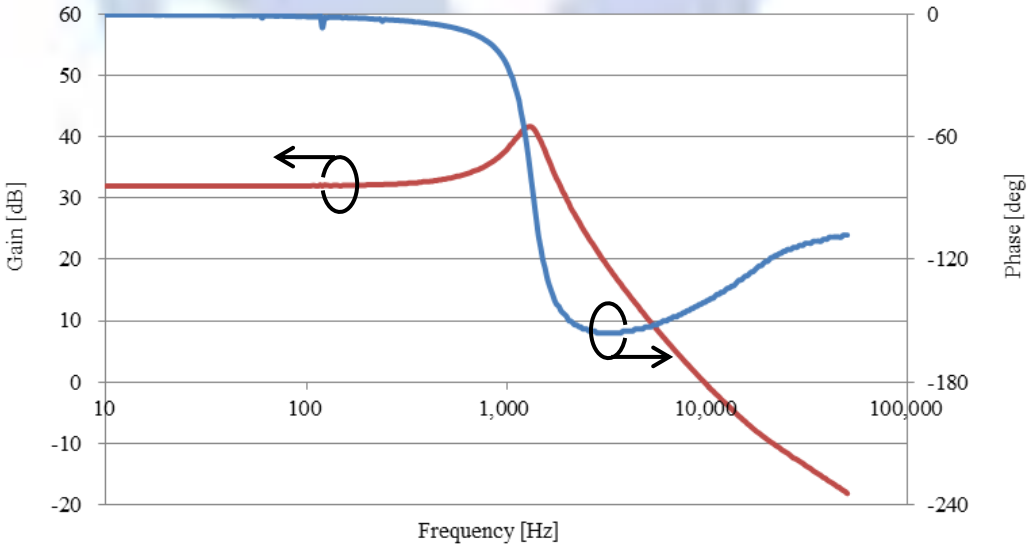

(b) I_2= - 4 A

Fig. 9. Frequency characteristics of G_{dv} (experimental results, buck-based type).

5. Transient Response

To investigate the transient characteristics response of the converter; two prototype 100 watts converters are designed based on the proposed seamless model. One of these converters is a buck-based type, while the other is a boost-based type. Each converter is connected, at one side, to a battery, and at the other side, to a bipolar current source. The current waveform of the bipolar current source, I_2, is intentionally designated to have a stiff change from positive I_2 into negative I_2.Accordingly, the voltage at the bipolar current source side V_2 is measured.The voltage of the current source is fedback to control the duty ratio of the switch S_M. The open loop transfer function *T(s)* becomes:

$$T(s) = K_p \cdot G_c(s) \cdot G_{dv}(s)$$

where;

K_p : Feedback proportional gain
$G_c(s)$: Transfer function of compensator

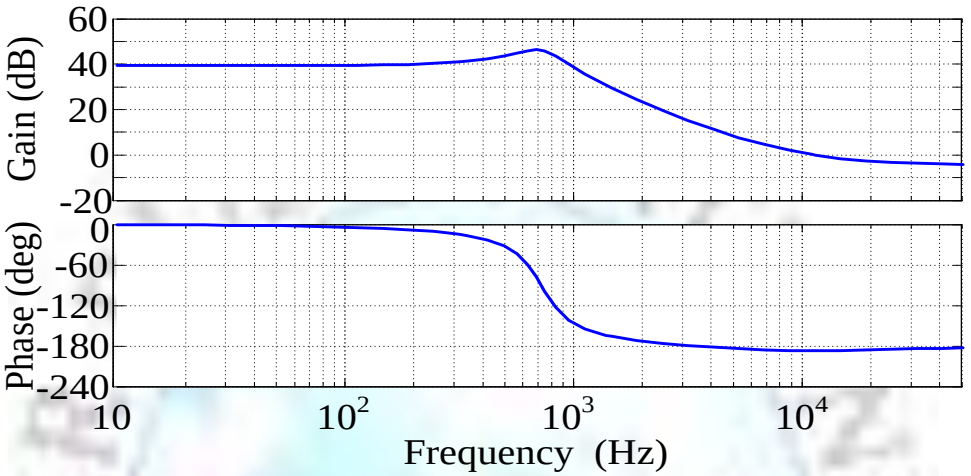

(a) I_2= +2 A

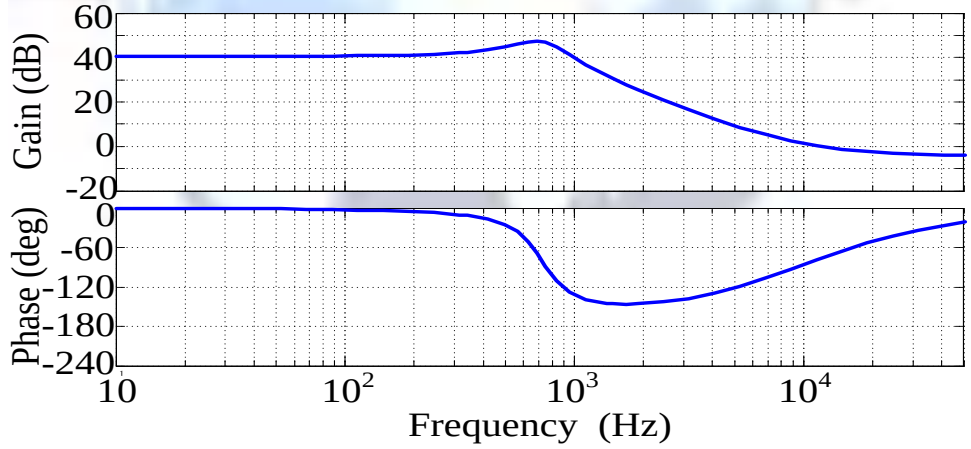

(a) I_2= - 2 A

Fig. 10. Frequency characteristics of G_{dv} (analytical results, boost-based type).

- For the buck-based type:

A compensator is not needed in buck-based type because its phase doesn't inverse. Compensator's transfer function in buck-based type becomes:

$$G_{c\_buck}(s) = 1$$

Proportional gain is designed as K_{p_buck}= 0.72 [V^{-1}].

The simulated results are shown in Fig.12, while the experimental results are shown in Fig.13. It is noticed that the experimental results and the simulated results are conformed. Also, it is clear that the transient change in V_2 (when the I_2 change from positive to negative) is the same transient change in V_2 (when the I_2 change from negative to positive). This, in turn, confirms that the buck-based type does not depend on the direction of I_2.

- For the boost-based type:

A compensator is needed in boost-based type because its phase does inverse when direction of I_2 is positive. In this circuit, phase lag compensator is used. Compensator's transfer function in boost-based type becomes:

$$G_{c\_boost}(s) = \frac{1 + \omega_p/s}{1 + \omega_z/s}$$

where;

=4.4 krad/s
= 30 rad/s

Proportional gain is designed as K_{p_boost}= 0.36 [V^{-1}].

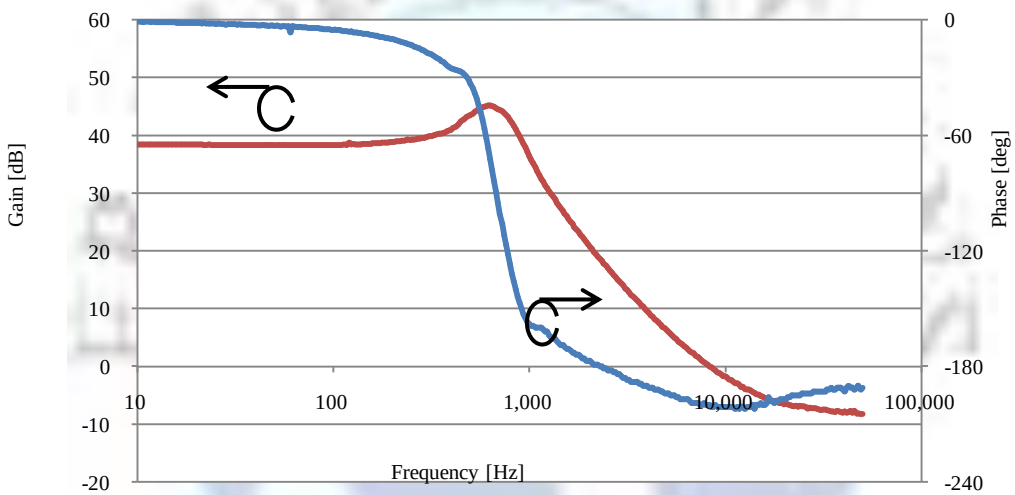

(a) I_2= +2 A

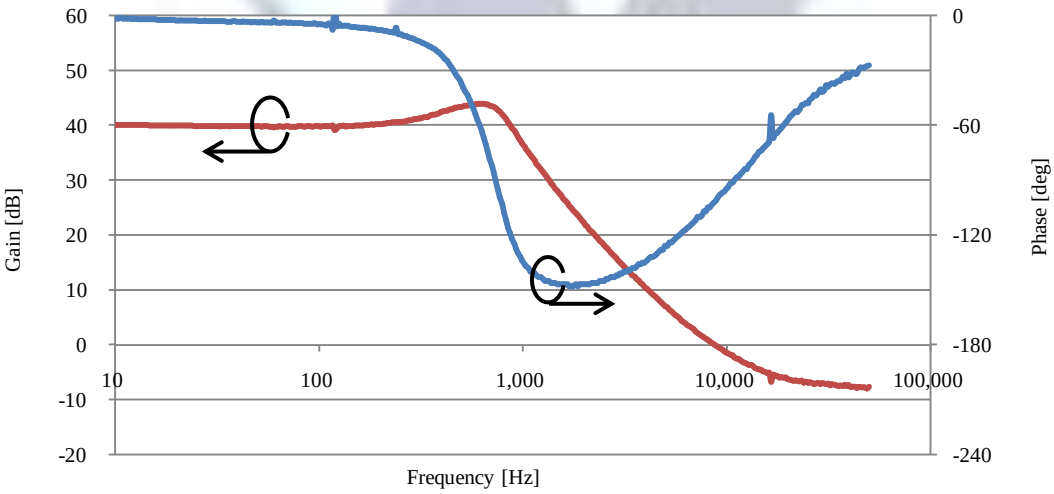

(b) I_2= - 2 A

Fig. 11. Frequency characteristics of G_{dv}(experimental results, boost-based type)

The simulated results are shown in Fig. 14, while the experimental results are shown in Fig.15. It is noticed that the experimental results and the simulated results are the same. Furthermore, it is clear that the transient change in V_2 (when the I_2 change from positive to negative) is higher than the transient change in V_2 (when the I_2 change from negative to positive). This, in turn, confirms that the buck-based type depends on the direction of I_2.

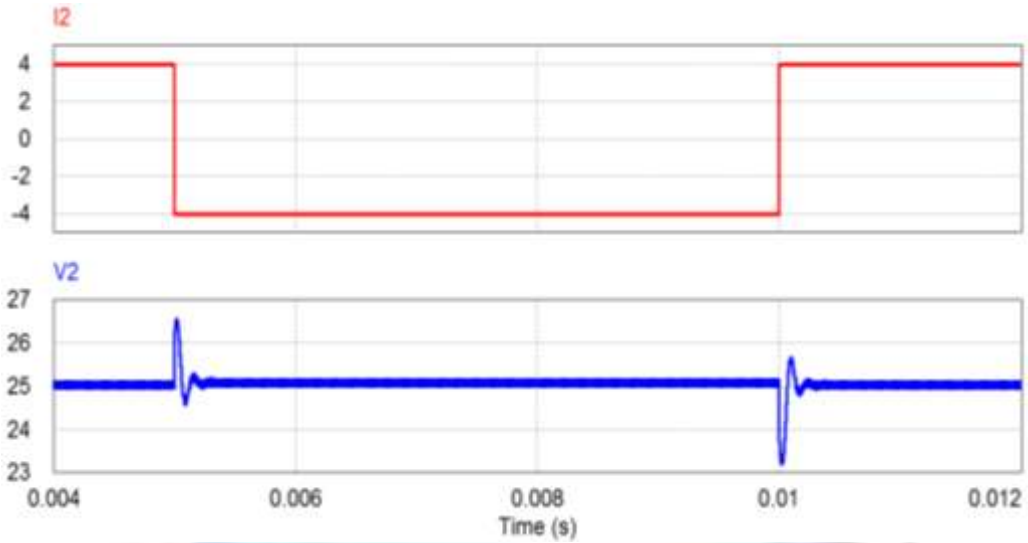

Fig. 12.Transient response characteristics of buck-based type(simulated result).

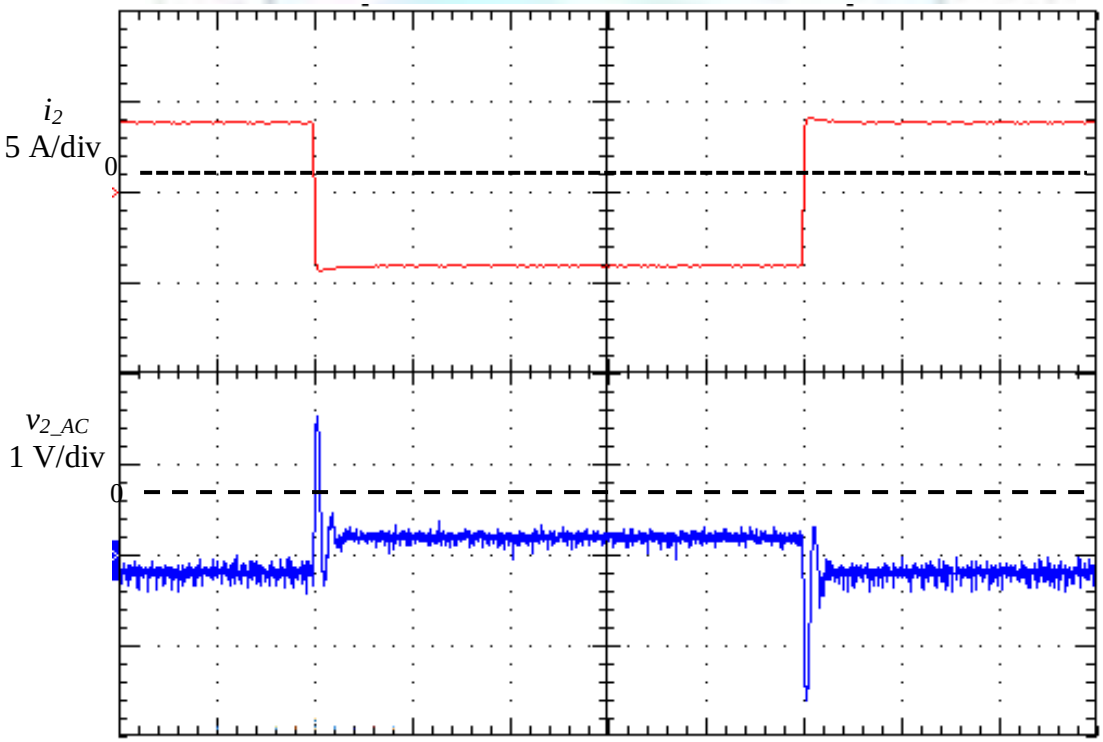

Fig. 13. Transient response characteristics of buck-based type (experimental result, time: 1ms/div).

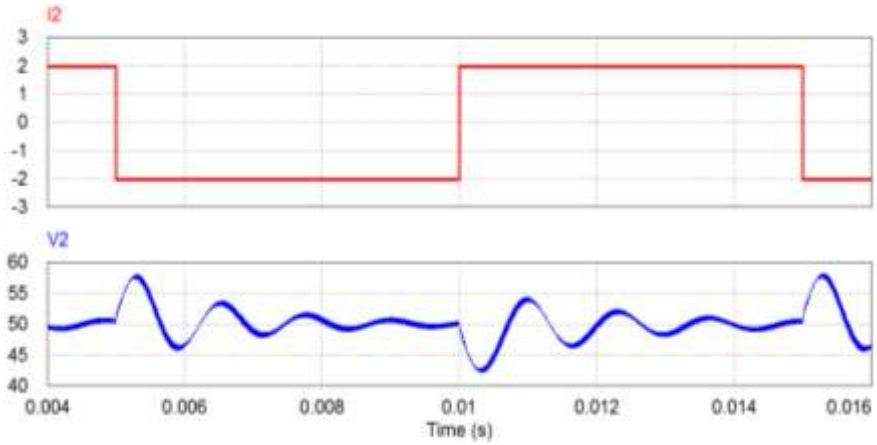

Fig. 14.Transient response characteristics of boost-based type (simulated result)

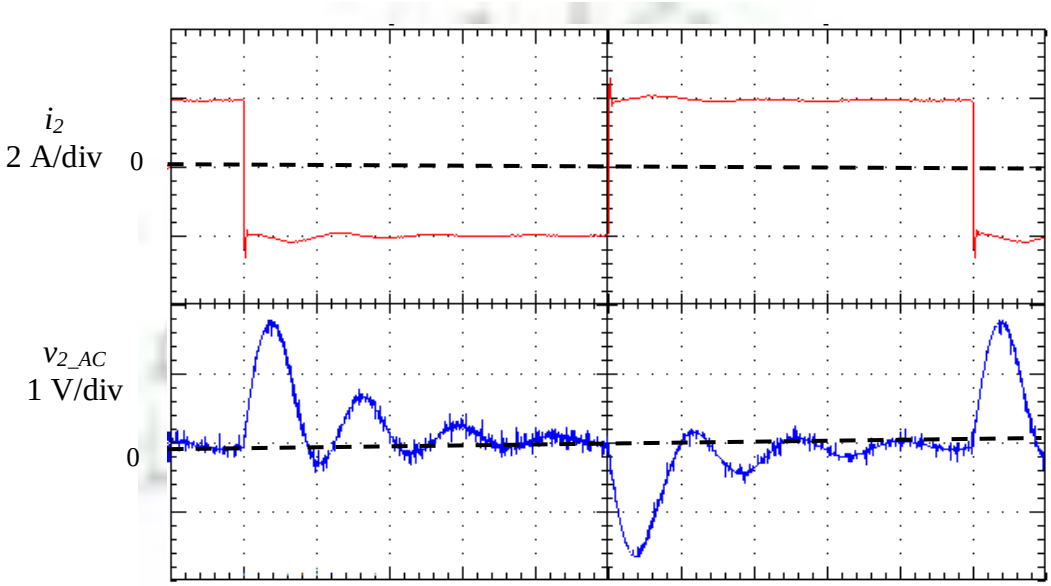

Fig. 15. Transient response characteristics of boost-based type (experimental result, time: 1ms/div)

6. Conclusion

A unified model for bi-directional DC-DC converters for both directions of power flow is introduced in this paper. This unified model is a seamless dynamic model in which the bidirectional DC-DC converter is connected, at one side, to an independent voltage source and, at the other side, to independent current source. The direction of the power flow is designated by the polarity of the independent current source. This seamless dynamic model is applied to two DC-DC converter circuits (buck-based type and boost-based type).

In case of boost-based type, its frequency characteristics depend on the direction of the current I_2. However, in case of buck-based type, its frequency characteristics don't depend on the direction of the current I_2. A simulated and experimental prototype for both circuits (buck-based type and boost-based type) are build up based on this seamless dynamic model, and their results are compered. Both of the simulated and experimental results support the seamless dynamic model idea and prove its superiority.

References

[1]. A. Payman, S. Pierfederici, and F. Meibody-Tabar,"Energy Management in a Fuel Cell/Supercapacitor Multisource/Multiload Electrical Hybrid System,"Power Electronics, IEEE Transactions on , vol.24, no.12, pp.2681,2691, Dec. 2009.

[2]. W. Liu, J. Chen, T. Liang, R. Lin, and C. Liu,"Analysis, Design, and Control of Bidirectional Cascoded Configuration for a Fuel Cell Hybrid Power System,"Power Electronics, IEEE Transactions on , vol.25, no.6, pp.1565,1575, June 2010.

[3]. J. Bauman and M. Kazerani, " A comparative study of feul-cell-battery-ultracapacitorvechicles," IEEE Trans. Veh. Technol., vol.57, no.2, pp.760-769, March 2008.

[4]. J. Gurrero, L. Vicuna, and J. Uceda, "Uninterruptible power supply systems provide protection" IEEE Ind. Electronic. Mag. 1 (1), pp.28-38, 2007.

[5]. S. Yang, K. Goto, Y. Imamura, and M.Shoyama,"Dynamic Characteristics Model of Bi-directional DC-DC Converter Using State-Space Averaging Method, "INTELEC 2012, 19.2, pp.1-5, Oct.2012.

[6]. H. A. Ramadan, Y. Imamura, K. Kawachi, S. Yang, and M.Shoyama,"Multi-level Virtual Conductor Using Bidirectional DC-DC Converters, " INTELEC2013, pp.105-109, 13-17 Oct. 2013.

[7]. D. M. Bellur and M. K. Kazimierczuk, "DC-DC Convertersfor Electric Vehicle Applications," EEIC2007, pp.286 – 293.

[8]. R. Li, A. Pottharst, N. Frohleke, and J. Bocker, "Analysis and Design of Improved Full-Bridge Bidirectional DC-DC Converter," IEEE PESC Cof. Rec.2004, pp. 521-526.

[9]. D. Liu and H. Li, "Dynamic Modeling and Control Design for Bidirectional DC-DC Converter for Fuel Cell Vehicles with Battery as Energy Storage Element", IAS 2005, Vol. 3, pp.1632 – 1635, Oct. 2005.

[10]. S. Cuk, "Modeling, Analysis, and Design of Switching Converter," Ph. D. thesis, California Institute of Technology, November 1976.

[11]. R. D. Middlebrook and S. Cuk, "Modeling and Analysis Methods for Dc-to-Dc Switching Converters," Proceedings of the IEEE International Semiconductor Power Converter Conference1977, pp. 90-111, March 1977. Reprinted in Advances in Switched-Mode Power Conversion, Vol. 1, Irvine: Teslaco, 1983.

[12]. T. Ninomiya, M. Nakahara, T. Higashi, and K. Harada, "A Unified Analysis of Resonant Converters," IEEE Transactions on Power Electronics, Vol. 6. No. 2. April 1991, pp. 260-270.